First-principle study on phase $Al_{0.8}Ni_3Sn_{0.2}$ in Sn–Ni–Al alloy as anode for lithium ion battery*

Huang Zhao-Wen(黄钊文)[a], Hu She-Jun(胡社军)[a]†,
Hou Xian-Hua(侯贤华)[a], Zhao Ling-Zhi(赵灵智)[b],
Ru Qiang(汝 强)[a], Li Wei-Shan(李伟善)[b], and Zhang Zhi-Wen(张志文)[a]

[a] *School of Physics and Telecommunication Engineering, South China Normal University, Guangzhou* 510006, *China*
[b] *Key Laboratory of Electrochemical Technology on Energy Storage and Power Generation of Guangdong Higher Education Institutes, South China Normal University, Guangzhou* 510006, *China*

(Received 4 January 2009; revised manuscript received 18 June 2010)

The mechanism of lithium intercalation/deintercalation for phase $Al_{0.8}Ni_3Sn_{0.2}$ as anode material used in lithium ion battery was studied carefully based on the first-principle plane wave pseudo-potential method. The calculated results indicated that Sn–Ni–Al alloy had high theoretical capacity when used as anode material, however, there was high initial irreversible capacity loss because of the large volume expansion. Therefore the technological parameters during preparing the Sn–Ni–Al anode should be controlled strictly to make the content of $Al_{0.8}Ni_3Sn_{0.2}$ phase as low as possible and to make the anode consist of promising Sn–Ni and Al–Ni phases. For comparison, an experiment based on magnetron sputtering was done. The result showed that the calculation is in good agreement with the experiment. We found that the first-principle investigation method is of far-reaching significance in synthesising new commercial anode materials with high capacity and good cycle performance.

Keywords: Sn–Ni–Al alloy, first-principle, lithium ion battery
PACC: 7115A, 8640H

1. Introduction

Lithium ion batteries are considered as one of the most important power sources owing to the advantages of high energy density and long cycle life.[1] The current anode materials used in commercial lithium ion batteries are graphite, whose theoretical capacity is low, 372 $mA \cdot h \cdot g^{-1}$,[2] and previous research has indicated that carbon anode materials have large irreversible capacity loss due to solid electrolyte interphase (SEI) film formed by the reaction between anode materials and the electrolyte.[3] Sn is considered as an alternative anode to graphite because it has high theoretical capacity, 994 $mA \cdot h \cdot g^{-1}$,[4] however, the cyclic stability of Sn is poor because of the considerable volume change during the charge/discharge process, resulting in the pulverisation of the anode material. The stability of Sn can be improved to some extent by synthesising active–inactive or active–active phase system, such as Sn–Ni alloy,[5−7] Sn–Cu alloy,[8−10] Sn–Co alloy[11−13] and Sn–Zn–Cu.[14] But, can the capacity be reduced by the use of alloys?

Recently, we have reported that Sn–Al anode had a high capacity because both Sn and Al were active for lithium intercalation/deintercalation,[15] but its capacity is floating and the cyclic stability needs to be improved. Meanwhile, from our former work,[8,16] Ni atoms can reunite with each other and provide a stable framework during the lithium intercalation/deintercalation because of the strong Ni covalent bonds, which benefit the cyclic stability. The purpose of this paper is to understand the stability improvement of Sn–Al by forming Sn–Ni–Al alloy through theoretic investigation based on the first-principle plane wave pseudo-potential method.

2. Computation method and crystal structure

2.1. Computation method

All of the calculations are based on density functional theory (DFT),[17−19] which is developed from the Thomas–Fermi model by Hohenberg and Kohn. Using functional variation to find the best form of

*Project supported by the National Natural Science Foundation of China (Grant No. 50771046), China Postdoctoral Science Foundation (Grant No. 20080440764), and Guangdong Province Natural Science Foundation (Grant No. 9451063101002082).
†Corresponding author. E-mail: husj@scnu.edu.cn
© 2010 Chinese Physical Society and IOP Publishing Ltd

single electron state, we can obtain the Schrödinger equation of single electron

$$\left[-\frac{\nabla^2}{2m} + V_{\text{ext}}(\boldsymbol{r}) + V_{\text{xc}}(\boldsymbol{r}) + V_{\text{eff}}(\boldsymbol{r}, \rho(\boldsymbol{r}))\right]\varphi_n(\boldsymbol{r}) = \varepsilon_{\text{i}}\varphi_n(\boldsymbol{r}), \quad (1)$$

$$\rho(\boldsymbol{r}) = \sum_n a_n |\varphi_n(\boldsymbol{r})|^2. \quad (2)$$

In Eq. (1), the first term is effective kinetic energy, $V_{\text{ext}}(\boldsymbol{r})$ stands for external field potential, the third term $V_{\text{xc}}(\boldsymbol{r})$ is the exchange correlation potential and the last term $V_{\text{eff}}(\boldsymbol{r}, \rho(\boldsymbol{r}))$ is effective potential. In Eq. (2), $\rho(\boldsymbol{r})$ stands for the density of electron states in the system, and a_n is the number of intrinsic electron states which have been taken.

In all of the calculations, exchange correlation energy is approximated by the generalised gradient approximation (GGA) using Perdew–Wang (PW91) form.[20] And the exchange correlation energy can be defined as the function between charge density and grads:

$$E_{\text{xc}}^{\text{GGA}}[\rho] = \int f_{\text{xc}}[\rho(\boldsymbol{r}), |\nabla\rho(\boldsymbol{r})|]\,\mathrm{d}r. \quad (3)$$

The interactions between valence electrons and ions are described by the ultrasoft Vanderbilt-type pseudo-potentials[21] supplied by Kresse and Hafner. Pseudo-wave is made as soft as possible to obtain the smallest cut-off energy. In the present work, all of the calculations are carried out based on Cambridge serial total energy package (CASTEP) in software Materials Studio 4.1 invented by Accelry company in America. The Brillouin zone integration is approximated by using the special k-point sampling scheme of Monkhorst–Pack. The $8 \times 8 \times 8$ k-point grid is used for phase $Sn_{0.2}Al_{0.8}Ni_3$, $6 \times 6 \times 6$ grid for phase $LiSn_{0.2}Al_{0.8}Ni_3$, $4 \times 4 \times 4$ grid for phase $Li_xSn_{0.2}Al_{0.8}Ni_3$ (x = 9–11), and $3 \times 3 \times 3$ grid for $Li_{12}Sn_{0.2}Al_{0.8}Ni_3$. The energy cutoff of plane-wave is set at 300 eV. Meanwhile, to obtain the most stable crystal structure and predigest the calculation, geometric optimisations on the crystal cell are done with the method of Broyden Flecher–Goldfarb–Shanno (BFGS) before calculation.

2.2. Crystal structure

Ni atoms added into Sn–Al alloy may react with its components to form Sn–Ni–Al ternary phases, or binary phases Sn–Ni and Al–Ni alloy phases. In this work, we will study carefully the Sn–Ni–Al alloy to understand the stability improvement of Sn–Al alloy. According to the ICSD2005, there is only one stable phase in Sn–Ni–Al alloy, namely, $Al_{0.8}Ni_3Sn_{0.2}$ phase. And the crystal structure of the phase is shown in Fig. 1.

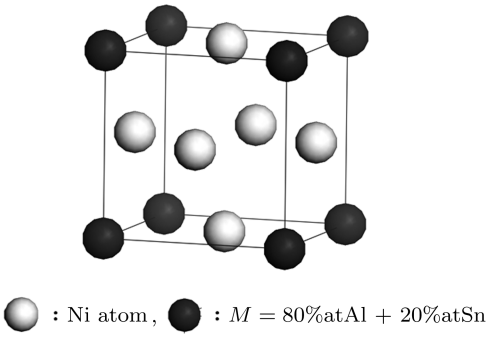


Fig. 1. The crystal structure of $Al_{0.8}Ni_3Sn_{0.2}$ phase.

The $Al_{0.8}Ni_3Sn_{0.2}$ phase belongs to $AuCu_3$ type structure, its space group is $Pm\bar{3}m$ and the lattice parameter is $a = b = c = 0.63$ nm. Ni atoms occupy (0, 0.5, 0.5) sites, which are distributed according to the symmetry. Sn and Al are located at the eight vertexes of the cube, which are composed of 80at%Al and 20at%Sn. The unit cell is depicted in Fig. 1.

According to intercalation/deintercalation kinetics, it can be assumed that the lithium atoms firstly fill in the octahedral and then the tetrahedral voids. After all of the interstitial sites are occupied, lithium atoms begin replacing the Ni atoms at the face-centred sites, according to Eqs. (4) and (5), the formation energies are given by Eqs. (6) and (7). The expansion ratio and theoretical capacity are given by Eqs. (8) and (9), respectively, where F is Faraday constant, ε is the geometry structural coefficient of materials and M is the relative molecular weight of the anode materials.

$$Al_{0.8}Ni_3Sn_{0.2} + xLi = Li_xAl_{0.8}Ni_3Sn_{0.2}, \quad (0 < x \leq 9); \quad (4)$$

$$Al_{0.8}Ni_3Sn_{0.2} + xLi - (x-9)Ni = Li_xAl_{0.8}Ni_{3-(x-9)}Sn_{0.2}, \quad (9 < x \leq 12); \quad (5)$$

$$E = -\frac{1}{x}[E_{\text{total}}(Li_xAl_{0.8}Ni_3Sn_{0.2}) - E_{\text{total}}(Al_{0.8}Ni_3Sn_{0.2}) - xE(Li_{\text{atom}})], \quad (0 < x \leq 9); \quad (6)$$

$$E = -\frac{1}{x}[E_{\text{total}}(\text{Li}_x\text{Al}_{0.8}\text{Ni}_{3-(x-9)}\text{Sn}_{0.2}) - E_{\text{total}}(\text{Al}_{0.8}\text{Ni}_3\text{Sn}_{0.2}) - xE(\text{Li}_{\text{atom}}) + (x-9)E(\text{Ni}_{\text{atom}})],$$
$$(9 < x \leq 12); \quad (7)$$

$$\eta = \frac{V - V_0}{V_0} \times 100\%; \quad (8)$$

$$C = \frac{x \cdot F}{\varepsilon \cdot M}. \quad (9)$$

According to Ref. [21], the lithium intercalation potential can be described by Eq. (10)

$$U \approx -\Delta E/\Delta x, \quad (10)$$

where ΔE is the change of the total energy after the reaction, and Δx is the change of the lithium concentration.

3. Theoretical calculations

3.1. Lithium intercalation process

There are two main ways for lithium intercalating in the metal or alloy. One is to intercalate into the host material by way of inserting between the occupied sites. For instance, in the case of using Sn as anode, the lithium intercalation process is as follows: $\text{Sn}+x\text{Li} = \text{Li}_x\text{Sn}$.[22] The other is in the way of taking the face-centred sites by replacing the host atoms. In the case of Sn_2Fe as the anode for example, lithium intercalation process is $\text{Sn}_2\text{Fe}+8.8\text{Li} = 2\text{Li}_{4.4}\text{Sn}+\text{Fe}$.[23] During the intercalation process, it is assumed that the crystal structure of the host materials does not change.

As for $\text{Al}_{0.8}\text{Ni}_3\text{Sn}_{0.2}$, its crystal structure is face-centred cubic (Fig. 2(a)). When it is used as an anode, lithium may first intercalate into the host by occupying the voids of the octahedrals and the tetrahedrals forming $\text{Li}_9\text{Al}_{0.8}\text{Ni}_3\text{Sn}_{0.2}$, as shown in Fig. 2(b). On the other hand, lithium may intercalate into the host by replacing Ni at the face-centred sites forming $\text{LiAl}_{0.8}\text{Ni}_2\text{Sn}_{0.2}$ because the bond energy between Sn and Al at the vertexes is larger than that between Sn (or Al) and Ni, as shown in Fig. 2(c). In this work, we first study these two lithium intercalation ways to understand the lithium intercalation mechanism.

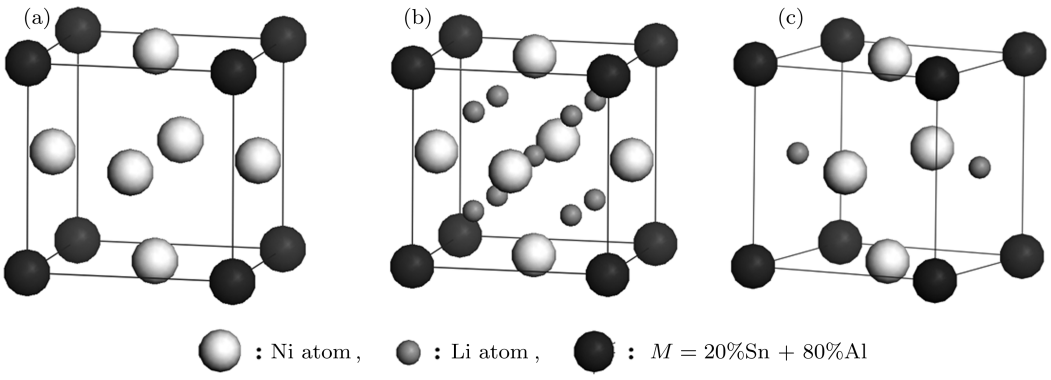


Fig. 2. Crystal structures of $\text{Al}_{0.8}\text{Ni}_3\text{Sn}_{0.2}$ (a), $\text{Li}_9\text{Al}_{0.8}\text{Ni}_3\text{Sn}_{0.2}$ (b) and $\text{LiAl}_{0.8}\text{Ni}_2\text{Sn}_{0.2}$ (c).

Table 1 lists the total energy and formation energy for phase $\text{Al}_{0.8}\text{Ni}_3\text{Sn}_{0.2}$ and the phases after undergoing the two intercalating ways. It can be seen that when lithium atoms are inserted into host materials in the way of intercalating into the interstitial sites, the formation energy is positive, that is, there is a certain energy given out during this process. However, when the lithium atoms intercalate in the way of replacing the Ni atoms, the formation energy is negative, namely, it would need certain energy for the phase to form. According to the discussion above, we can draw a conclusion that replacing reaction is impossible to exist before all of the interstitial sites are taken. Consequently, the lithium atoms inserted into the host material will first intercalate the interstitial sites of octahedral and tetrahedral voids. Once the energy is accumulated enough to destroy the Ni–Sn/Al bond, lithium atoms will keep replacing the Ni atoms at the face-centred sites, and the Ni atoms replaced will stay in the host material in free-state.

Table 1. Total energy and formation energy of $Al_{0.8}Ni_3Sn_{0.2}$, $Li_9Al_{0.8}Ni_3Sn_{0.2}$ and $LiAl_{0.8}Ni_2Sn_{0.2}$.

samples	total energy/eV	formation energy/eV
$Al_{0.8}Ni_3Sn_{0.2}$	–4139.7877	–
$Li_9Al_{0.8}Ni_3Sn_{0.2}$	–5846.3978	1.6005
$LiAl_{0.8}Ni_2Sn_{0.2}$	–2973.3247	–7.4481

3.2. Computation result and analysis

The structures of phases $Li_xAl_{0.8}Ni_3Sn_{0.2}$ (x = 0, 1, 9) and $Li_xAl_{0.8}Ni_{3-(x-9)}Sn_{0.2}$ (x = 10, 11, 12) are shown in Fig. 3, whose calculated electrochemical parameters are listed in Table 2.

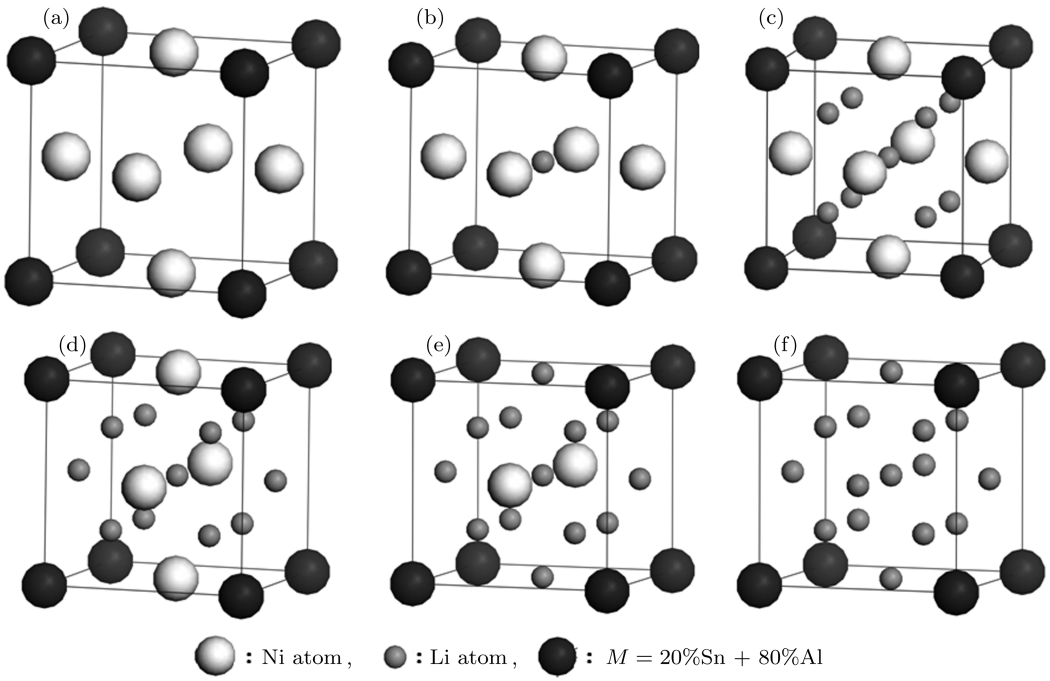


Fig. 3. Crystal structures of $Li_xAl_{0.8}Ni_3Sn_{0.2}$. (a) $Al_{0.8}Ni_3Sn_{0.2}$ x = 0, (b) Li $Al_{0.8}Ni_3Sn_{0.2}$ x = 1, (c) Li_9 $Al_{0.8}Ni_3Sn_{0.2}$ x = 9 and $Li_xAl_{0.8}Ni_{3-(x-9)}Sn_{0.2}$, (d) $Li_{10}Al_{0.8}Ni_2Sn_{0.2}$ x = 10, (e) $Li_{11}Al_{0.8}NiSn_{0.2}$ x = 11, (f) $Li_{12}Al_{0.8}Sn_{0.2}$ x = 12.

Table 2. Electrochemical parameters of $Li_xAl_{0.8}Ni_3Sn_{0.2}$.

samples	total energy/eV	formation energy/eV	cell volume /$\times 10^{-3}$ nm^3	expansion ratio/%	capacity/mA · h · g^{-1}	U/V
$Al_{0.8}Ni_3Sn_{0.2}$	–4139.7877	–	46.1449	–	–	–
$Li_9Al_{0.8}Ni_3Sn_{0.2}$	–5846.3978	1.6005	244.4475	429.7391	1089.5207	1.6005
$Li_{10}Al_{0.8}Ni_2Sn_{0.2}$	–4681.3542	0.8376	238.1245	416.0364	817.9124	0.8376
$Li_{11}Al_{0.8}NiSn_{0.2}$	–3515.2090	0.1133	270.7969	486.8404	1096.0195	0.1133
$Li_{12}Al_{0.8}Sn_{0.2}$	–2349.3299	–0.4682	309.0193	569.6716	1529.3664	0.4682

Figure 4 describes the relationship between the formation energy and the lithium concentration. Obviously, the formation energy decreases as the lithium concentration increases, that is, the energy given out during the lithium intercalation process decreases as more lithium atoms are inserted into the host material, which indicates that it is more and more difficult for the lithium atoms to be inserted into the host material. Furthermore, when the lithium concentration is small ($x \leq 11$), the formation energy is positive, namely, there is a certain energy to be given out at the lithium intercalation reaction and it is easy for the lithium atoms to insert into these sites. However, when the lithium concentration grows larger ($x = 12$),

the formation energy becomes negative, which means that it would need certain energy for the phase to form during the lithium intercalation process. On the other hand, the value of this negative formation energy is small, which can be easily accumulated during the following charge/discharge process, therefore, the phase is also possible to be formed. Consequently, it can be said that the description of the lithium intercalation process is reasonable.

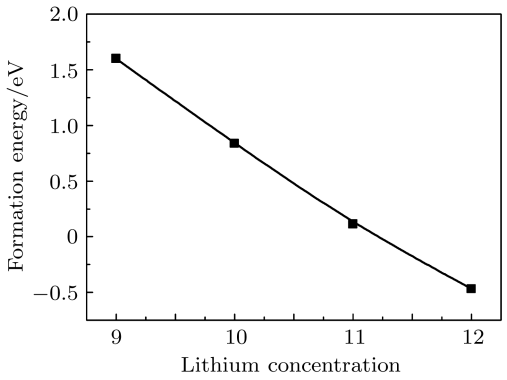


Fig. 4. The relationship between the formation energy and the lithium concentration.

Figure 5 depicts the relationship among lithium concentration, expansion ratio and theoretical capacity, from which we can find that the volume expansion increases quickly when the lithium atoms are inserted into the host material in the way of intercalating the interstitial sites. After the lithium atoms occupy all of the interstitial sites ($x = 9$), the material will expand greatly (the expansion ratio is 429%). However, as the lithium atoms start to replace the Ni atoms at the face-centred sites, the volume expansion slows down (when $x = 10$, the expansion is 416%), which would decrease the volume change and benefit to the cycle performance. With the replacement of Ni atoms, the volume keeps expanding.

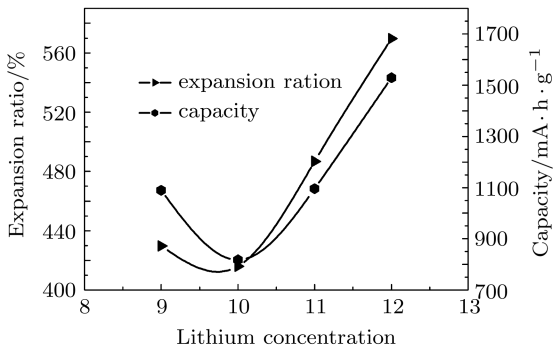


Fig. 5. The relationship among lithium concentration, expansion ratio and theoretical capacity.

Meanwhile, the changing trend of the theoretical capacity is similar with the volume expansion ratio. When all of the interstitial sites are occupied, the theoretical capacity reaches 1089 $\mathrm{mA \cdot h \cdot g^{-1}}$. However, when the lithium atoms start to replace the Ni atoms, the capacity will decrease slightly. As the replacing reaction continues, the theoretical capacity increases quickly. When all of the Ni atoms are replaced, the capacity reaches 1529 $\mathrm{mA \cdot h \cdot g^{-1}}$.

According to the discussion above, when the lithium atoms start to replace the Ni atoms at the face-centred sites, the bond length gets shorter, and the force between the atoms grow stronger. The lithium atoms which replace the Ni atoms and inhabit the face-centred sites could not overcome the force between the atoms and could not escape easily, leading to an irreversible capacity loss. This is the main reason why the capacity becomes decreased when the Ni atoms is replaced by the lithium atoms initially.

From our point of view, although the phase $Al_{0.8}Ni_3Sn_{0.2}$ has a high theoretical capacity, as the lithium concentration increases, the volume expansion which reaches 429% has pulverised the anode material, resulting in a high initial irreversible capacity loss. Therefore the technological parameters during preparing the Sn–Ni–Al anode should be controlled strictly to make the content of $Al_{0.8}Ni_3Sn_{0.2}$ phase as low as possible and try to make the anode consist of promising Sn–Ni and Al–Ni phases such as Ni_3Sn_4.

Consequently, Sn–Ni–Al alloy used as anode materials improves the cycle performance at the cost of irreversible capacity loss and it is an incompatible problem for most of the investigated alloy electrode materials that the high reversible capacity and good cycle performance cannot be satisfied at the same time.

4. Experimental

For comparison, based on magnetron sputtering, we have investigated the $Al_{0.8}Ni_3Sn_{0.2}$ alloy used as an anode material in experimental aspect. Cu foil was used as substrate body. We chose $Al_{0.8}Ni_3Sn_{0.2}$ alloy target (purity 99.99%) in the experiment. The film was sputtered at RF frequency for 20 min, with power 175 W. Electrochemical tests were performed in CR2016 button cell with pure lithium metal foil as cathode, Celgard-2300 as the separator and $LiPF_6$ (1 mol/L) in EC (ethylene carbonate) + DMC (dimethyl carbonate) + EMC (ethyl methyl carbonate) with 1 : 1 : 1 volume ratio as electrolyte. The

cells were assembled in an argon-filled glove box. Cyclic voltammogram test were carried out in Solartron SI1260 electrochemistry system at a scan rate of 0.5 mV/s.

From Fig. 6(b), we can find that there are current peaks at about 0.1 V, 0.4 V, 0.8 V and 1.75 V respectively. The peak at 1.75 V moves to about 1.6 V after the first cycle. Consequently, we can draw a conclusion that the experimental result is consistent with the calculated one (Fig. 6(a)). The peak at about 0.8 V which is considered to be formed by phase $Li_{10}Al_{0.8}Ni_2Sn_{0.2}$ did not appear after the first cycle, indicating that the lithium atoms cannot escape after intercalating into this site and it is consistent with the analysis in Fig. 5. From our point of view, besides the formation of the solid electrolyte interphase (SEI) film,[24] the formation of phase $Li_9Al_{0.8}Ni_3Sn_{0.2}$ also contributes to the peak at 1.75 V, because the lithium intercalation potentials are close to each other. This may be the reason why at so small a lithium concentration the peak is sharpest. Also, because the SEI film leads to high loss of active lithium ions, the peak at 1.75 V weakens greatly after the first cycle. Furthermore, from the cyclic voltammogram curve, all of the peaks weaken quickly after the first cycle, which shows that there is a large initial capacity loss. It is consistent with the analysis of the calculated result. Consequently, we can come to the conclusion that the calculated result is in good agreement with the experimental one.

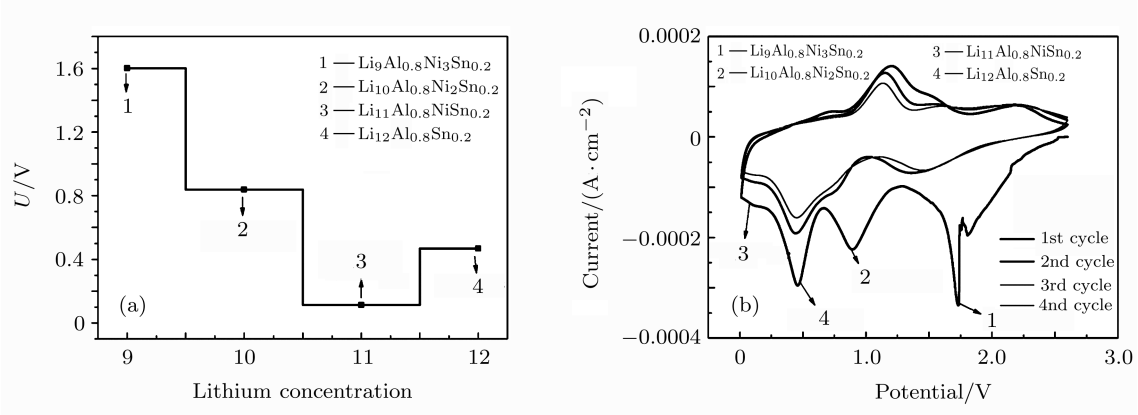


Fig. 6. The comparison between the calculated potential and the cyclic voltammogram test result. (a) the calculated potential, (b) the cyclic voltammogram test result.

5. Conclusion

In this work, based on the first-principle plane wave pseudo-potential method, we have carried out an in-depth study on the mechanism of lithium inserting/escaping when Sn–Ni–Al alloy is used as anode materials for lithium ion battery. The calculated results indicated that although the $Al_{0.8}Ni_3Sn_{0.2}$ phase used as an anode material has high theoretical capacity up to 1529.3664, it presents large initial irreversible capacity loss due to the large volume expansion (more than 400%). Therefore the technological parameters during preparing the Sn–Ni–Al anode should be controlled strictly to make the content of $Al_{0.8}Ni_3Sn_{0.2}$ phase as low as possible and to make the anode composed of promising Sn–Ni and Al–Ni phases such as Ni_3Sn_4. Consequently, Sn–Ni–Al alloy used as anode materials improves the cycle performance at the cost of irreversible capacity loss. For comparison, an experiment based on magnetron sputtering was done. The result showed that the calculation is in good agreement with the experimental result. And we found that the first-principle plane wave pseudo-potential method is efficient in predicting the character of new anode materials. It is of far-reaching significance in synthesising new commercial anode materials with high capacity and good cycle performance.

References

[1] Bruo S 1995 *Nature* **373** 557

[2] Megahed S and Scrosati B 1994 *J. Power Sources* **51** 79

[3] Wang C, Galobardes F and Madou M 2006 *Diamond and Related Materials* **15** 1930

[4] Nishikawa K, Fukunaka Y, Sakka T, Ogata Y and Selman J R 2007 *J. Power Sources* **174** 668

[5] Lee H Y, Jang S W, Lee S M, Lee S J and Baik H K 2002 *J. Power Sources* **112** 8

[6] Ehrlich G M, Durand C, Chen X, Hugener T A, Spiess F and Suib S L 2000 *J. Electrochem. Soc.* **147** 886

[7] Hou X H, Hu S J, Li W S, Zhao L Z and Yu H W 2008 *Rare Metal Materials and Engineering* **37** 827 (in Chinese)

[8] Wang K, He X M, Wang L, Ren J G, Jiang C Y and Wan C R 2006 *J. Electrochem. Soc.* **153** 1859

[9] Larcher D, Beaulieu L Y, Macneil D D and Dahn J R 2000 *J. Electrochem. Soc.* **147** 1658

[10] Hou Z F, Liu H Y, Zhu Z Z, Huang M C and Yang Y 2003 *Acta Phys. Sin.* **52** 952 (in Chinese)

[11] Ke F S, Huang L, Wei H B, Cai J S, Fan X Y, Yang F Z and Sun S G 2007 *J. Power Sources* **170** 450

[12] Tamura N, Fujimoto A, Kamino M and Fujitani S 2004 *Electrochim. Acta* **49** 1949

[13] Valvo M, Lafont U, Simonin L and Kelder E M 2007 *J. Power Sources* **174** 428

[14] Kitamura S, Wang L, Tanase S, Obata K and Sakai T 2003 *Electrochemistry* **71** 1070

[15] Yu H W, Hu S J, Hou X H, Ru Q, Chen T J and Li W S 2009 *Materials Science Forum* **610–613** 467

[16] Hou X H, Hu S J, Li W S, Ru Q, Yu H W and Huang Z W 2008 *Chin. Phys.* B **17** 3422

[17] Jones R O and Gunnarsson O 1989 *Rev. Mod. Phys.* **61** 689

[18] Dreizler R M and Gross E K U 1990 *Density Functional Theory* (Berlin: Springer Vertag)

[19] Becke A D 1988 *Phys. Rev.* A **38** 3098

[20] Perdew J P, Chevary J A, Vosko S H, Jackson K A, Pederson M R, Singh D J and Fiolhais C 1992 *Phys. Rev.* B **46** 6671

[21] Vanderbilt D 1990 *Phys. Rev.* B **41** 7892

[22] Hou X H, Hu S J, Li W S, Zhao L Z, Yu H W and Tan C L 2008 *Acta Phys. Sin.* **57** 2374 (in Chinese)

[23] Mao O, Dunlap R A, Courtney I A and Dahn J R 1998 *J. Electrochem. Soc.* **145** 4195

[24] Fan X Y, Zhuang Q C, Jiang H H, Huang L, Dong Q F and Sun S G 2007 *Acta Phys. Chim. Sin.* **23** 973 (in Chinese)